УДК 544.47;546.215;546.655

A. Grinko, A. Brichka, O. Bakalinska, S. Brichka, M. Kartel

CATALASE MIMETIC ACTIVITY OF KAOLIN CLAY DECORATED WITH NANOSIZED CERIUM OXIDE

A series of kaolin nanomaterials decorated with CeO_2 was synthesized by reaction of cerium nitrate deposition in an aqueous medium without stabilizers at room temperature. Amount of deposited cerium oxide in nanomaterial vary from 2.76 % to 7.37 %. The size of CeO_2 nanocrystalls was established and vary from 5.6 till 10.4 nm. X-ray analysis of samples shown that deposited cerium dioxide has a cubic structure. IUVSCe4+/IUVSCe3+ ratio in nanocomposites were evaluated by UV diffuse reflection spectroscopy. The catalytic activity of the synthesized materials, kaolin, pure cerium nanoxide was investigated in a model reaction of hydrogen peroxide decomposition in pH range 8.5–0.5 and compared with the enzyme catalase activity. It was proven that the activity of ceria oxide decorated catalysts correlates with modifier content. The dependence of the samples Ce-5K, Ce-7K, Ce-9K and CeO_2 nano activity on pH is extreme with maximum at pH 9.5–10. Catalase mimetic activity of the studied materials in terms of 100 % content of cerium oxide CeO_2 correlates with nanooxide particle dispersion and ceria surface defects evaluated as IUVSCe4+/IUVSCe3+ ratio.

Keywords: kaolin clay, nanosized cerium oxide, catalase mimetic activity, hydrogen peroxide decomposition.

Introduction

Nanotechnology – one of the most promising fields in modern science and technology. Nanomedicine applies the features and objects of nanotechnology to diagnose and treat diseases, or improve biological functions of the body. Nanocrystalline materials like cerium dioxide widely used in nano medicine biotechnology. Nanoscale particles of CeO_2 are potent antioxidants (protect against oxygen active forms like oxygen ions, free radicals, organic and inorganic peroxide compounds) in cell culture models [1], are also used to treat severe skin burns [2], as potential therapeutic agents for glaucoma and blindness [3], to protect tissues from radiation damage [4], are promising for prevention and treatment of Alzheimer's disease, Parkinson's, Huntington, redox therapy of malignant tumors [5]; for proliferation and growth of stem cells. Studies have shown that nano-CeO_2 can be active similar to the enzymes superoxide dismutase or catalase [6].

The reason for CeO_2 intensive study and use is its unique redox behavior. Nanoparticles of cerium dioxide, unlike oxide particles of large size, have a much larger number of surface defects [7]. These defects are mainly surface oxygen vacancies, causing a change in the local electron and valence environment, which stabilizes the oxidation state Ce^{3+}.

The aim of this work is the modification of kaolin by cerium dioxide for obtaining new nanocomposites kaolin / cerium oxide, the study of their physical and chemical properties, experimental determination and comparison of the catalytic catalase-mimetic activity of the synthesized materials in a model reaction of hydrogen peroxide decomposition with activity of the enzyme catalase, kaolin and commercial pure cerium nanooxide at different pH of the reaction medium.

Materials and methods

Synthesis of nanocomposites was carried out by reaction of cerium nitrate deposition in an aqueous media without stabilizers at room temperature:

$$4Ce(NO_3)_3 + 12NaOH + O_2 = \\ = 4CeO_2 + 12NaNO_3 + 6H_2O.$$

Kaolin of P-2 "Dysten Limited" was used. The precipitate nanocomposites was filtered, washed and dried at 383 °C. Cerium oxide content in the samples was established by atomic emission spectrometry (ICPE-9000, Shimadzu). Nanocomposites were characterized by TEM (Hitachi H-800) with the use of electron diffraction in the selected area. The particle size was determined on the images in the dark field using the linear measurements of a sample of more than 40 objects for each sample. Nanocomposites characterized by SEM (MIRA3 LMU, TESCAN) with energodispersive spectroscopic chemical analysis Oxford X-MAX 80 mm^2 device with uncertainty of ± 1 %. Nanomaterials IR spectra were registered at room temperature on spectrometer

Thermo Nicolet IR Nexus FT-IR in 4000–400 cm^{-1} diapason, in diffuse reflectance measurement mode with uncertainty of ± 1.8 cm^{-1}. Nanocomposites UV-Vis spectra were registered on UV-VIS-NIR spectrophotometer UV-3600, Shimadzu device in diffuse reflection mode in the range of 220–800 nm with uncertainty of ± 1 nm. The crystalline structure of synthesized cerium nanooxide was determined by electron- and X-ray diffraction. X-ray analysis was performed on diffractometer DRON-4-07.

Catalase mimetic activity of investigated materials was estimated by monitoring the catalytic hydrogen peroxide (HP) decomposition. Volumetric method used to determine the kinetic of HP decomposition [8]. For analysis, quantitative assessment and comparison of catalase mimetic activity of nanomaterials and enzyme catalase, Michaelis constant (Km, mM) have been applied. Maximal reaction rate was calculated from kinetic curves for different substrate (HP) concentration (1–11 %). The graph of reaction speed dependence from substrate concentration in inverse Lainuivere–Berck coordinates allow to calculate Michaelis constants. Affinity constants (Kaf, reverse to Michaelis constant, mM^{-1}) has been applied for easy interpretation of experimental data. The influence of pH value (borate buffer pH 8.5–10.5) on the catalytic activity was investigated.

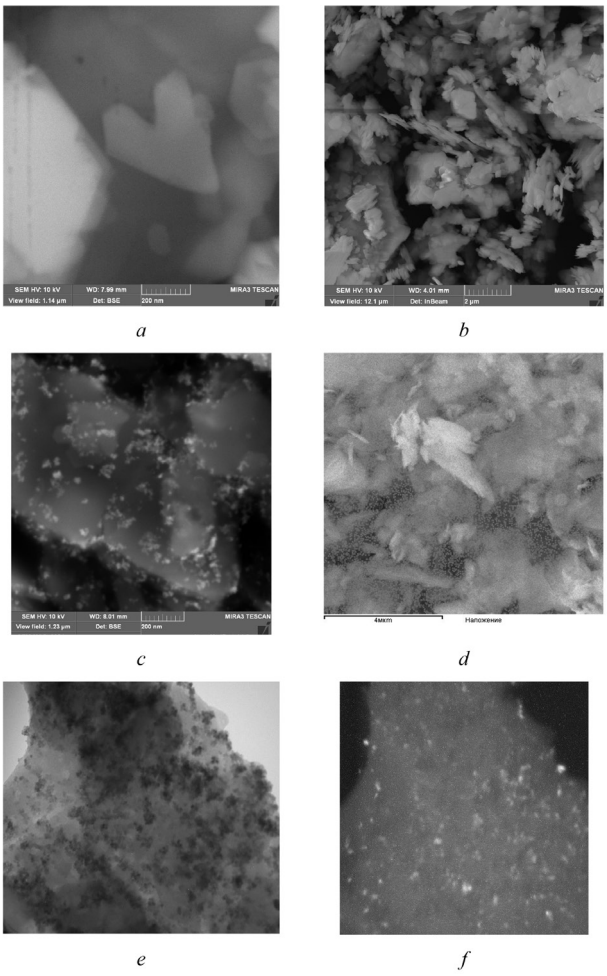

Fig. 1. SEM (*a, b, c, d*) and TEM (*e, f*) images of kaolin (*a, b*) and Ce-9K nanocomposite, *d* – distribution of CeO_2 in material

Results and discussion

Normally to obtain nanoscale inorganic particles it is needed carefully select conditions of synthesis – reagent concentration, speed of the components addition and mixing, pH, temperature of synthesis, templates application, and others. Our experience shows that nanoscale particles of ceria can be produced in a wide range of content (20 %) from dilute solutions without a significant influence of other factors [9–12]. Cerium oxide content in the samples according atomic emission spectrometry, are presented in Table 1. The results of chemical analysis indicate that the content of cerium oxide in the samples compared with the calculated is lower, probably due to CeO_2 leaching during filtration stage.

It is known that the nanocomposite dispersion and cerium oxide particles distribution in the kaolin matrix affects the biological activity of the material. SEM image demonstrate that the kaolin particle size in samples ranging from hundreds of nanometers to tens of micrometers (Fig. 1, *a–d*). Nanoscale particles observed in images of nanocomposites after modification. Analysis of the SEM and SEM images of identical samples makes it possible to argue that are cerium dioxide particles. Cerium dioxide nanoparticles uniformly distributed in an array of modified kaolin. TEM images of modified kaolin (Fig. 1, *e*, *f*) are represented in bright and dark fields. Much smaller in size and different

Table 1. **CeO_2 content and its particle size, $I_{UVS\ Ce}^{4+}/I_{UVS\ Ce}^{3+}$ in nanocomposite**

Material	CeO_2 content, %	Average particle diameter, nm	$I_{UVS\ Ce}^{4+}/I_{UVS\ Ce}^{3+}$ in UV spectra of nanocomposite
Ce-3K	2.76 ± 0.01	5.6	0.98
Ce-5K	4.55 ± 0.02	6.9	1.33
Ce-7K	6.16 ± 0.02	8.6	2.11
Ce-9K	7.37 ± 0.04	10.4	2.88
CeO_2 nano	100.00	31.0	–

morphology objects are observed on large particles, which is especially noticeable on TEM images in a dark field.

Image analysis of nanocomposites with different content of cerium oxide demonstrates the increase of content and modifier particle size. The increase in the concentration of the modifier under nanocomposite synthesis process leads to the formation of particles of larger size. The dependence of the average value of particle diameters of cerium dioxide content is practically linear (Fig. 2).

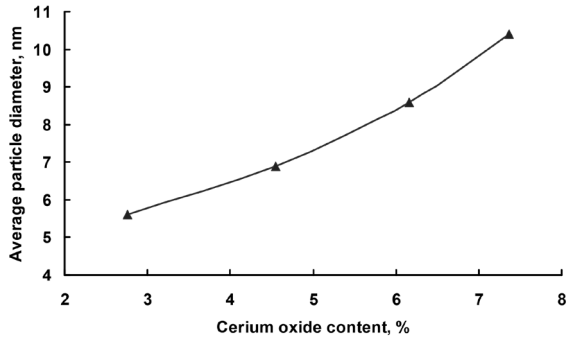

Fig. 2. The dependence of the ceria oxide particle size on its content in the nanocomposites according to electron microscopy

The nanocomposites particles electron diffraction study found the reflexes with d(hkl) = 3.12 (111), 2.7 (200), 1.89 (220) and 1.64 Å (311), which indicate cubic structure of ceria (Fig. 3). Significant blurring of the signal modifier can be explained by the nanoscale effect and low crystallinity of the cerium dioxide [9].

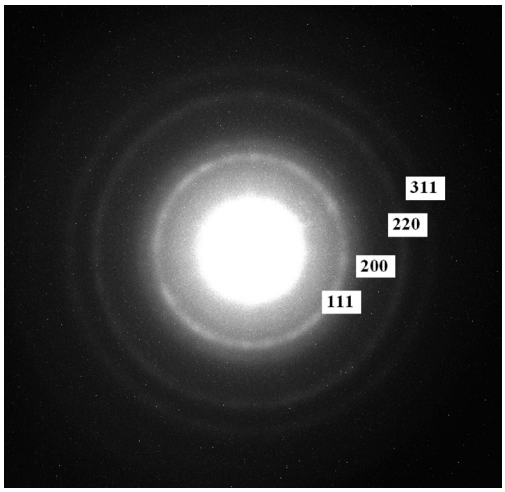

Fig. 3. Electronograms of CeO_2 particle in nanocomposite – d(hkl) = 3.12 (111), 2.7 (200), 1.89 (220) i 1.64 Å (311)

IR spectra of nanocomposites have no significant differences from kaolin spectra (Fig. 4). We can see absorption bands of hydroxyl groups at 3750–3600 cm^{-1}, adsorbed water at 3550–3400 cm^{-1}, and below 1200 cm^{-1} bands of kaolin frame Al–O and Si–O connections. Cerium dioxide is not active in IR spectra. Between the modifier and the matrix is no chemical interaction which would impact on the vibrational spectra of modified kaolin.

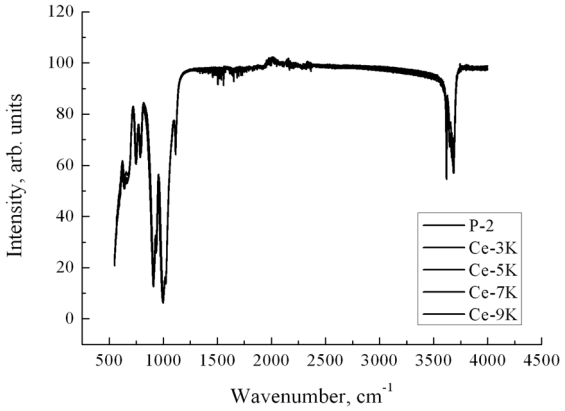

Fig. 4. Nanocomposite IR spectra

Catalytic, biological, including physiological activity of cerium dioxide defined as oxide crystallite size and Ce^{4+}/Ce^{3+} ratio. Three types of electronic transitions are characteristic of cerium: between configuration f↔d, intraconfiguration f↔f and transitions with charge transfer. Question of the contribution of different valence cerium atoms (cerous – Ce (III) and ceric – Ce (IV)) in the total broad band of cerium oxide UV spectra is debatable. Two possible alternatives describes in the literature: according to the first long-wavelength peak attributed to Ce^{3+}, short-wave peak to Ce^{4+}. For example, in [13], a spectra with the absorption bands of Ce^{3+} and Ce^{4+} at 330 and 240 nm, respectively described. These bands are due to 4f–5d transitions [14]. Similar dependence observed in the emission spectra [15]. The absorption bands maxima in the UV spectra of the cerium oxide glass observed at 4.48 eV (277 nm) for the Ce^{3+} and 5.15 eV (241 nm) for Ce^{4+} [16]. According to the second point of view long-wavelength peak attributed to Ce^{4+} while short-wave peak to Ce^{3+} [17; 18]. These data are confirmed by XPS studies [19]. Three- and four valence cerium ions have different spectral characteristics [18]. Probably, further investigations help determine the contribution of different valence cerium atoms. The ratio of the peaks intensities is not an atomic ratio and serves as a qualitative measure of the change in the contribution of different valence cerium atoms. Tetravalent cerium in the UV range have signal at approximately 400 nm, which corresponds to the charge transition $O^{2-}(2p) \rightarrow Ce^{4+}(4f)$. The signal overlaps with an electronic transition $5d^1 \rightarrow 4f^1$ of Ce^{3+}ions. Normally, defects in the form of trivalent

cerium determined the structure of ceria. Their appearance is due to low energy $Ce^{3+} \leftrightarrow Ce^{4+}$ transition. It is possible that oxidation of cerium (III) hydroxide is not complete during the synthesis of nanocomposite. Ce^{3+} ions embedded in the crystal structure of cerium dioxide instead Ce^{4+} as defects and spectral shift $O^{2-}(2p) \rightarrow Ce^{3+}(4f)$ observed about 250 nm [18]. We investigated UV diffuse reflectance spectra of kaolin and synthesized cerium containing nanocomposites (Fig. 5). A number of maximums (most intense at 251.5 nm), which attribute to impurities of iron, titanium, aluminum silicate and others are identified on the spectrum of unmodified kaolin. Modification of kaolin brings to the spectrum signal of cerium dioxide. The maximums of intense signal at 284.5 (Ce-3K), 290 (Ce-5K), 290.5 (Ce-7K) and 292.5 (Ce-9K) nm shift in the long-wavelength side with rising of cerium oxide content (Fig. 5), confirming the observations of the authors [18].

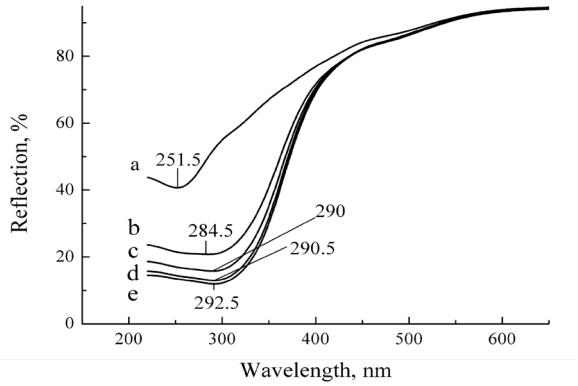

Fig. 5. UV spectra of kaolin (*a*) and nanocomposites Ce-3K (*b*), Ce-5K (*c*), Ce-7K (*d*), Ce-9K (*e*)

Modifier (cerium oxide) profiles were determined as the difference between the UV spectra of nanocomposites and kaolin. The spectrum of modifier was decomposed by Gauss in two components for four- and trivalent cerium. With increasing the size of the ceria particles in nanocomposites modifier absorption maxima are shifted to the red region to the values of 250 and 400 nm, which are characteristic of Ce^{4+} and Ce^{3+} signal ceria. $I_{UVS\ Ce}{}^{4+}/I_{UVS\ Ce}{}^{3+}$ ratio was calculated as the ratio of integrated intensities of signals (Table 1). These data are necessary to find the correlation between the structural parameters of the nanocomposite and its catalytic (biological) activity. Obviously, the number of ions Ce^{3+} decreases with increasing of cerium oxide content in nanocomposites. We can assume that Ce^{3+} is surface defects and increase the size of the nanocrystals in the nanocomposite led to CeO_2 crystallites surface and number of surface defects decreases.

Literature data have shown that the preparations of cerium exhibit enzyme-mimetic (superoxiddismutase- and catalase-like) activity [6]. In the present work, the authors evaluated and compared the catalytic ability of the synthesized nanocomposites with the enzyme catalase in the model reaction of hydrogen peroxide decomposition from positions of formal kinetics of enzymatic reactions – calculation of Michaelis constant from kinetics data of substrate (hydrogen peroxide) decomposition. Catalase mimetic activity of kaolin, nanocomposites with different CeO_2 content (samples Ce-3K, Ce-5K, Ce-7K, Ce-9K), commercial pure cerium nanooxide (CeO_2 nano) and enzyme catalase was investigated in model reaction of hydrogen peroxide decomposition.

Since it is impossible to foresee the weight of the catalyst which gives the maximum reaction rate, we determined it experimentally from kinetic data of the hydrogen peroxide decomposition by different weight catalyst. Line interval of dependence of the maximum rate of hydrogen peroxide decomposition from catalyst sample mass was determined in the range 0–0.035 g. For further experimental

Table 2. **Michaelis constants (mM) and value of reliability approximation R^2**

Catalyst	Km, mM; (R^2)				
	pH = 8.5	pH = 9.0	pH = 9.5	pH = 10.0	pH = 10.5
Catalase	476 (0.99)	480 (0.99)	526 (0.99)	520 (0.98)	645 (0.99)
CeO_2 nano	70 (0.98)	60 (0.98)	20 (0.98)	119 (0.95)	45 (0.99)
Kaolin	520 (0.97)	410 (0.98)	482 (0.90)	918 (0.99)	1738 (0.99)
Ce-3K	202 (0.97)	194 (0.99)	193 (0.98)	189 (0.95)	219 (0.94)
Ce-5K	164 (0.92)	152 (0.99)	135 (0.99)	144 (0.85)	188 (0.93)
Ce-7K	160 (0.98)	143 (0.97)	108 (0.98)	98 (0.99)	133 (0.92)
Ce-9K	158 (0.99)	127 (0.99)	78 (0.98)	55 (0.96)	87 (0.99)

determination of Michaelis constant data, 0.025 g sample of catalyst was chosen from linear interval. Similar determining were made for another nanocomposites, nano-sized cerium oxide and the enzyme catalase

Michaelis constant were calculated from kinetic data of hydrogen peroxide (concentrations 1 %; 3 %; 5 %; 7 %; 9 %; 11 %) decomposition. The true concentration of the original solution set by titrimetric method. Optimal weight of the catalyst was added to the 25 ml of resulting solution. Changes in the concentration of hydrogen peroxide at the time determined by periodic fixing the volume of oxygen released from the reaction media by volumometric method.

Dependence of Km on pH and reliability of approximation value R^2 are in Table 2 for investigated catalyst, Kaf – pH in Fig. 6.

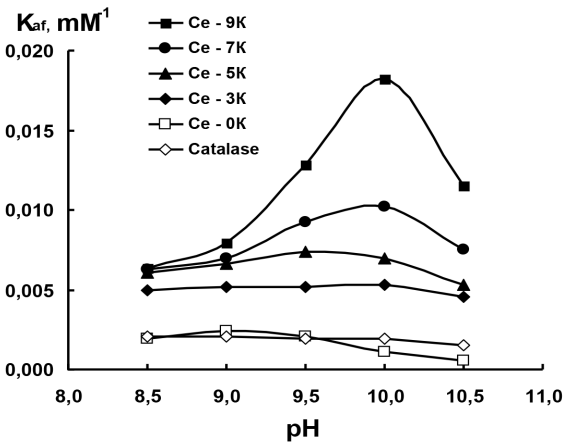

Fig. 6. The dependence of materials activity on pH

Nanosized CeO_2 is most active among the studied catalysts. His Michaelis constant for pH 9.5 is 20 mM, which is almost 26 times bigger than this value for the enzyme catalase under these conditions. Activity of cerium containing materials correlates with the content of cerium oxide. The dependence of the activity materials Ce-5K, Ce-7K, Ce-9K on pH is extreme with maximum at pH 9.5–10. The analysis of the values of affinity constants suggests a linear dependence of the catalytic activity of the nanomaterial on nanosized cerium oxide content in it (Fig. 6).

The activity of the studied materials, attributed to the content of cerium oxide shows that the most active material is Ce-3K sample containing 2.8 % of modifier. Its activity in 1.45 times higher than the commercial pure nanooxide cerium one. This can be attributed to the size of cerium oxide nanocrystals deposited in material. For Ce-3K sample CeO_2 nanoparticles diameter is the smallest of all samples and is 5.6 nm, while for the commercial CeO_2 sample particle diameter is 31 nm (Fig. 7).

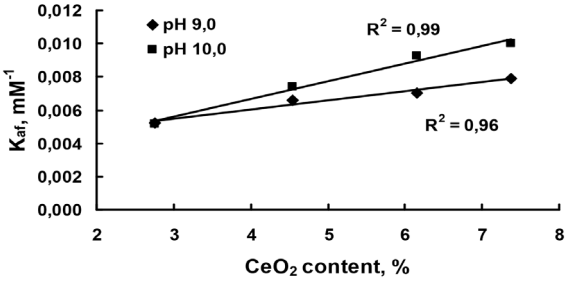

Fig. 7. Linear dependence of nanomaterials activity on CeO_2 content

It is very important to understand which parameter of modifier (CeO_2) in nanocomposite correlate with its catalytic activity. For this purpose we recalculate the activity of studied materials in terms of 100 % content of cerium oxide. It was shown that the most active material is Ce-3K sample containing 2.8 % of modifier. Its activity in 1.45 times higher than the nanooxide cerium one. This can be attributed to the size of cerium oxide nanocrystals deposited in material. For Ce-3K sample CeO_2 nanoparticles diameter is the smallest of all samples and is 5.6 nm, while for the commercial CeO_2 sample particle diameter is 31 nm (Fig. 8). Smoler nanocrystalites in nanocomposite have higher dispersion and $I_{UVSCe}{}^{4+}/I_{UVSCe}{}^{3+}$ ratio (Table 1).

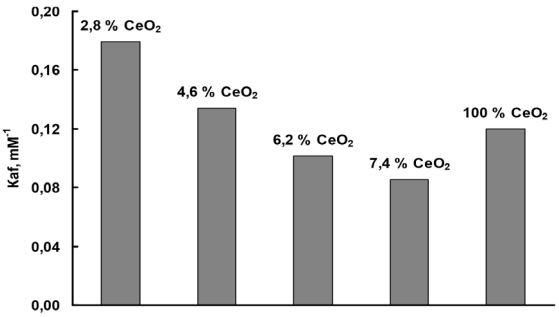

Fig. 8. Catalytic activity of nanomaterials in terms of 100 % content of nanosized CeO_2

Conclusions

A series of kaolin nanomaterials decorated with CeO_2 was synthesized by reaction of cerium nitrate deposition in an aqueous medium without stabilizers at room temperature. Amount of deposited cerium oxide in nanomaterial very from 2.76 till 7.37 %. The size of CeO_2 nanocrystalls was established and vary from 5.6 till 10.4 nm. X-ray analysis of samples shown that deposited cerium dioxide has a cubic structure. $I_{UVSCe}{}^{4+}/I_{UVSCe}{}^{3+}$ ratio in nanocomposites were evaluated by UV diffuse reflection spectroscopy. The catalytic activity of the

synthesized materials, kaolin, pure cerium nanooxide was investigated in a model reaction of hydrogen peroxide decomposition in pH range 8.5–10.5 and compared with the enzyme catalase activity. It was shown that the activity of cerium oxide decorated catalysts correlates with modifier content. The dependence of the samples Ce-5K, Ce-7K, Ce-9K and CeO_2 nano activity on pH is extreme with maximum at pH 9.5–10. Catalase mimetic activity of studied materials in terms of 100 % content of cerium oxide CeO_2 correlate with nanooxide particle dispersion and ceria surface defects, evaluated as $I_{UVSCe}^{4+}/I_{UVSCe}^{3+}$ ratio. So, synthesized nanocomposites are effective catalyst and can be used in biotechnology and medicine for peroxide substances decomposition.

References

1. The potential toxic effects of cerium on organism: cerium prolonged the developmental time and induced the expression of Hsp70 and apoptosis in Drosophila melanogaster / B. Wu, D. Zhang, D. Wang [et al.] // Ecotoxicology. – 2012. – Vol. 21. – P. 2068–2077.
2. Kuchma M. H. Phosphate ester hydrolysis of biologically relevant molecules by cerium oxide nanoparticles / M. H. Kuchma, J. Colon, A. Teblum // Nanomedicine: Nanotechnology, Biology, and Medicine. – 2010. – Vol. 6. – P. 738–744.
3. Bakht M. A novel technique for simultaneous diagnosis and radioprotection by radioactive cerium oxide nanoparticles: study of cyclotron production of ^{137m}Ce / M. Bakht, M. C. Sadeghi, C. Tenreiro // J. Radioanal Nucl Chem. – 2012. – Vol. 292. – P. 53–59.
4. Chen H.-I. Synthesis of nanocrystalline cerium oxide particles by the precipitation method / H.-I. Chen, H.-Y. Chang // Ceramics International. – 2005. – Vol. 31, № 6. – P. 795–802.
5. Wondrak G. T. Redox-directed cancer therapeutics: Molecular mechanisms and opportunities / G. T. Wondrak // Antioxid. Redox Signal. – 2009. – Vol. 11, Is. 12. – P. 3015–3055.
6. Tschtipe A. Catalytic redox activity and electrical conductivity of nanocrystalline non-stoichiometric cerium oxide / A. Tschtipe, J. Ying, C. M. Tuller // Sensors and Actuators. – 1996. – Vol. 31. – P. 111–114.
7. Exposure, health and ecological effects review of engineered nanoscale cerium and cerium oxide associated with its use as a fuel additive / F. R. Cassee, E. C. van Balen, C. Singh [et al.] // Rev. Toxicol. – 2011. – Vol. 41. – P. 213–229.
8. Каталітична активність церійвмісних матеріалів у реакції розкладання пероксиду водню / Т. Ю. Дмитренко, К. С. Кулик, К. В. Войтко [та ін.] // Хімія, фізика та технологія поверхні. – 2014. – Т. 5, № 3. – С. 317–324.
9. Decoration of carbon nanotubes with cerium (IV) oxide / S. Ya. Brichka, I. B. Yanchuk, A. A. Konchits [et al.] // ХФТП. – 2011. – Т. 2, № 1. – С. 34–40.
10. Влияние нековалентного модифицирования на структурные характеристики многослойных углеродных нанотрубок / Е. А. Ковальская, С. Я. Бричка, Н. Т. Картель [и др.] // Поверхность. – 2010. – Т. 2, № 17. – С. 205–213.
11. Формирование наночастиц оксида церия (IV) на поверхности углеродных нанотрубок / А. В. Бричка, И. Б. Янчук, Л. Ю. Котел [и др.] // Украинский химический журнал. – 2011 – Т. 77, № 3. – С. 17–20.
12. Модифицирование алюмосиликатных нанотрубок диоксидом церия / С. Я. Бричка, Л. Ю. Котел, Е. И. Оранская [и др.] // Украинский химический журнал. – 2013. – Т. 79, № 6. – С. 97–100.
13. Maeng J.-H. The Effect of Cerium Reduction on Light Emission in Cerium-containing $20Y_2O_3$-$25Al_2O_3$-$55SiO_2$ Glass / J.-H. Maeng, S.-Ch. Choi // Journal of the Optical Society of Korea. – 2012. – Vol. 16, № 4. – P. 414–417.
14. Методы определения разновалентных форм церия и европия (Обзор) / А. О. Стоянов, И. В. Стоянова, Н. А. Чивирева, В. П. Антонович // Методы и объекты химического анализа. – 2013. – Т. 8, № 3. – С. 104–118.
15. Preparation and optical properties of CeF_3-containing oxide fluoride glasses / H. Takahashi, S. Yonezawa, M. Kawai, M. Takashima // Journal of Fluorine Chemistry. – 2008. – Vol. 129, № 11. – P. 1114–1118.
16. Арбузов В. И. Основы радиационного оптического материаловедения : учеб. пособие / В. И. Арбузов. – СПб. : СПбГУИТМО, 2008. – 284 с.
17. Максимчук П. О. Формирование люминесцентных центров в нанокристаллах CeO_{2-x} : дис. … канд. физ.-мат. наук, 01.04.10 – физика полупроводников и диэлектриков / П. О. Максимчук. – Харьков, 2015. – 133 с.
18. Lin K. Synthesis, characterization, and application of 1-D cerium oxide nanomaterials: a review / K. Lin, S. Chowdhury // Int. J. Mol. Sci. – 2010. – № 1. – P. 3226–3251.
19. Tsunekawa S. X-ray photoelectron spectroscopy of monodisperse CeO_{2-X} nanoparticles / S. Tsunekawa, T. Fukuda, A. Kasuya // Surface Science. – 2000. – Vol. 457, Is. 3. – P. L437–L440.

Грінько А. М., Бричка А. В., Бакалінська О. М., Бричка С. Я., Картель М. Т.

КАТАЛАЗОПОДІБНА АКТИВНІСТЬ КАОЛІНУ, ДЕКОРОВАНОГО НАНОРОЗМІРНИМ ОКСИДОМ ЦЕРІЮ

Ряд наноматеріалів на основі каоліну, декорованих CeO_2, було синтезовано шляхом осадження нітрату церію у водному середовищі без стабілізаторів за кімнатної температури. Кількість депонованого оксиду церію в наноматеріалах становить 2,76–7,37 %. Було встановлено, що розмір CeO_2 у нанокристалітах варіюється від 5,6 до 10,4 нм. Рентгеноструктурний аналіз зразків показав, що діоксид церію має кубічну структуру. Співвідношення Ce^{4+}/Ce^{3+} в нанокомпозитах оцінювали за допомогою УФ-спектроскопії дифузного відбиття. Каталітичну активність синтезованих матеріалів, каоліну та чистого нанооксиду церію досліджували в модельній реакції розкладання пероксиду водню в інтервалі pH 8,5–10,5 і порівнювали з активністю ферменту каталаза. Було показано, що активність каталізаторів, декорованих оксидом церію, корелює з вмістом модифікатора.

Залежність активності зразків Се-5К, Се-7К, Се-9К і нано-CeO_2 від pH екстремальна з максимумом при pH 9,5–10. Каталазоподібна активність вивчених матеріалів у перерахунку на 100 % вміст оксиду церію корелює з дисперсністю часток нанооксиду та поверхневими дефектами, оціненими за відношенням $I_{UVSCe}{}^{4+}/I_{UVSCe}{}^{3+}$. Таким чином, синтезовані нанокомпозити є ефективними каталізаторами і можуть бути використані в біотехнології та медицині для розкладання пероксидних сполук.

Ключові слова: каолін, нанорозмірний оксид церію, каталазоподібна активність, пероксиду водню розкладання.

Матеріал надійшов 11.01.2016

УДК 678.674:616-089.843

Руденчик Т. В., Рожнова Р. А., Галатенко Н. А., Кісельова Т. О.

ВЛАСТИВОСТІ КОПОЛІМЕРІВ НА ОСНОВІ ОЛІГООКСИПРОПІЛЕНФУМАРАТУ, ДИМЕТАКРИЛАТ ТРИЕТИЛЕНГЛІКОЛЮ ТА N-ВІНІЛПІРОЛІДОНУ/СТИРОЛУ

Синтезовано кополімери на основі олігооксипропіленфумарату (ООПФ), диметакрилат триетиленгліколю (ТГМ-3) та N-вінілпіролідону (ВП) та кополімери на основі ООПФ, ТГМ-3 і стиролу (СТ) за різного вмісту ВП і СТ. Досліджено структуру синтезованих кополімерів та виявлено вплив ВП і СТ на їхні фізико-механічні та теплофізичні властивості. Встановлено, що потрійні кополімери зі стиролом мають більші показники модуля пружності при стисненні в порівнянні з кополімерами з ВП.

Ключові слова: олігооксипропіленфумарат, N-вінілпіролідон, стирол, кополімер.

Вступ

Завдяки біосумісності та здатності до біодеградації ненасичені олігоестери широко використовують при створенні полімерів медичного призначення [1–5].

До широко застосовуваних ненасичених олігоестерів при створенні матеріалів медичного призначення належать поліпропіленфумарати (ППФ), які отримують на основі діетилфумарату та 1,2-пропандіолу [2]. Наявність ненасиченого подвійного зв'язку забезпечує здатність ППФ утворювати монолітні зшиті структури, тоді як присутність естерних груп надає здатності до гідролітичної біодеградації з утворенням біосумісних фрагментів.

Введенням до структури зшитої полімерної системи на основі ППФ різних за властивостями компонентів можна отримували полімерні матеріали різного медичного призначення з покращеними властивостями.

Відома зшита полімерна матриця на основі ППФ та діетилфумарату, отримана під дією УФ-опромінення з використанням фотоініціатора